

Article

Investigations into NO_x Formation Characteristics during Pulverized Coal Combustion Catalyzed by Iron Ore in the Sintering Process

Junying Wan ^{1,2}, Tiejun Chen ^{1,2,*}, Xianlin Zhou ^{1,2,*} , Jiawen Liu ^{1,2}, Benjing Shi ³ , Zhaocai Wang ³ and Lanlan Li ⁴

¹ School of Resources and Environmental Engineering, Wuhan University of Science and Technology, Wuhan 430081, China; jywan92@163.com (J.W.); liujiawen0224@163.com (J.L.)

² Hubei Key Laboratory for Efficient Utilization and Agglomeration of Metallurgical Mineral Resources, Wuhan 430081, China

³ Zhongye Changtian International Engineering Co., Ltd., Changsha 410205, China; shi_benjing@126.com (B.S.); midrex@163.com (Z.W.)

⁴ Guangxi Beigang Resources Development Co., Ltd., Nanning 530201, China; lilanlan6299@163.com

* Correspondence: chentiejun@wust.edu.cn (T.C.); xlzhou@wust.edu.cn (X.Z.)

Abstract: Sintering accounts for about 50% of the total NO_x emissions of the iron and steel industry. NO_x emissions from the sintering process can be simulated using the emissions from coke combustion. However, the generation and emission law for NO_x burning in the sintering process of pulverized coal is still not clear. The formation characteristics of NO_x during coal combustion catalyzed by iron ore fines and several iron-containing pure minerals were studied in this paper. The results showed that iron ore fines can improve the NO_x emission rate and increase the total NO_x emissions during coal combustion. The type and composition of the iron ore fines have an important impact on the generation and emission of NO_x in the process of coal combustion. The peak concentration and emissions of NO_x in coal combustion flue gas with limonite, hematite or specularite added increased significantly. The peak value for the NO_x concentration in the coal combustion flue gas with magnetite or siderite added increased, but the emissions decreased. Therefore, the generation of NO_x in the sintering process can to a certain extent be controlled by adjusting the type of iron-containing raw materials and the distribution of the iron-containing raw materials and coal.

Keywords: iron ore sintering; NO_x formation; iron-containing pure minerals; coal combustion



Citation: Wan, J.; Chen, T.; Zhou, X.; Liu, J.; Shi, B.; Wang, Z.; Li, L. Investigations into NO_x Formation Characteristics during Pulverized Coal Combustion Catalyzed by Iron Ore in the Sintering Process. *Metals* **2022**, *12*, 1206. <https://doi.org/10.3390/met12071206>

Academic Editor: Liming Lu

Received: 6 May 2022

Accepted: 11 July 2022

Published: 15 July 2022

Publisher's Note: MDPI stays neutral with regard to jurisdictional claims in published maps and institutional affiliations.



Copyright: © 2022 by the authors. Licensee MDPI, Basel, Switzerland. This article is an open access article distributed under the terms and conditions of the Creative Commons Attribution (CC BY) license (<https://creativecommons.org/licenses/by/4.0/>).

1. Introduction

NO_x is one of the predominant pollutants in the iron and steel industry [1]. Sintering is a major emitter of pollutants in the steel industry, producing about 50% of the NO_x in this industry [2–4]. The emission of NO_x has caused great harm to human health and the living environment, such as acid rain, photochemical smog, etc. Therefore, there is an urgent need to reduce the emission of nitrogen oxides [5,6]. In China, the permitted hourly NO_x emission concentration since 2019 has been below 50 mg of NO_x/Nm³ (16% O₂) for the nose of a sintering machine.

Iron ore sintering is a basic agglomeration process providing sinter for blast furnaces. The sintering mixture (iron-containing raw materials, fuel, flux, return ore, etc.) is mixed with an appropriate amount of water and then paved on the sintering machine trolley after granulation. After the surface of the sintering material is ignited, the fuel inside the sintering material burns and releases heat from top to bottom under the forced suction of the lower bellows. The mixture undergoes a series of physical and chemical reactions under the action of high temperature and finally consolidates into sinter [7,8]. The solid fuels used in conventional sintering are mainly anthracite and coke [9]. NO_x can be divided into

three types according to its mechanism of formation: thermal NO_x , prompt NO_x and coal NO_x [10,11]. In the sintering process, NO_x mainly comes from coke breeze and anthracite combustion [12,13]. In addition, NO accounts for 95% of the total NO_x [14]. Therefore, NO_x emission from the sintering process could be simulated by that of coke combustion.

At present, most researchers have focused on source control, process control and end-of-pipe treatment technology for NO_x in sintering flue gas. Resource control mainly refers to the use of low-nitrogen coke and biomass carbon in the iron ore sintering process [15,16], the use of new low-nitrogen burners, etc. Process control mainly refers to control of sintering process parameters, sintering additives [5,17], fuel pretreatment [18], gas injection [19], flue gas circulation [20], etc. End-of-pipe treatment technologies include selective SNCR [21–23], SCR [24–26], activated carbon adsorption [27] and oxidative absorption [28]. However, the high gas flow rate, moisture content and dust concentration in the sintering flue gas lead to many problems with denitration technology, such as high operating costs and secondary pollution [12].

However, few studies have been published on the mechanisms of NO_x production in sintering so far [29]. Although the NO_x emissions from pulverized coal in boilers and in fluidized bed combustion have been fully investigated, the combustion process of coal in the sintering process is very different from fuels in coal-fired systems. In the sintering process, coal is mainly found in the combustion zone and the preheating zone [30], which together comprise a very complex gas, solid and molten liquid phase system, thus entailing a significant distinction in the reaction conditions and atmosphere of coal combustion compared to an ordinary coal combustion system [4]. Therefore, the reaction of NO_x generated by coal combustion in the sintering process is also different from that of the coal combustion system.

In recent years, several studies have investigated the emission and reduction of NO_x in the iron ore sintering process. Calcium ferrite formed in the high-temperature sintering zone has an impact on NO_x emission, catalyzing NO_x decomposition and reducing its emission level [29,31–34]. NO_x emissions decreased when a specially prepared coke containing CeO_2 was used during the iron ore sintering process [5]. The addition of Fe_3O_4 , FeO and Fe can reduce the generation and emission of NO_x in the sintering process [35,36]. Under certain conditions, the presence of CO seems to reduce NO_x , and this reduction reaction is catalyzed by sintered ore, Fe_2O_3 , Fe_3O_4 and MgO [37,38].

Although significant research has been carried out to analyze the generation of and reduction in emissions of NO_x in the sintering process, the generation and emission law for NO_x burning in the sintering process of pulverized coal is still not clear. This study focused on NO_x formation characteristics during pulverized coal combustion catalyzed by iron ore fines and several major iron-containing pure minerals in the iron ore sintering process.

2. Materials and Methods

2.1. Raw Materials

The main chemical composition of the iron ore fines obtained from a Chinese steel and iron group is shown in Table 1. The results showed that the iron grade of the iron ore fines was 61.47% and the loss on ignition was 5.14%. Proximate and ultimate analyses of coal (air-dry basis) are shown in Table 2. The nitrogen content in the pulverized coal was 0.645%. The fixed carbon mass fraction was 79.86%, and the ash and volatile matter were 15.06% and 3.63%, respectively.

Table 1. Chemical composition of raw materials/wt.%.

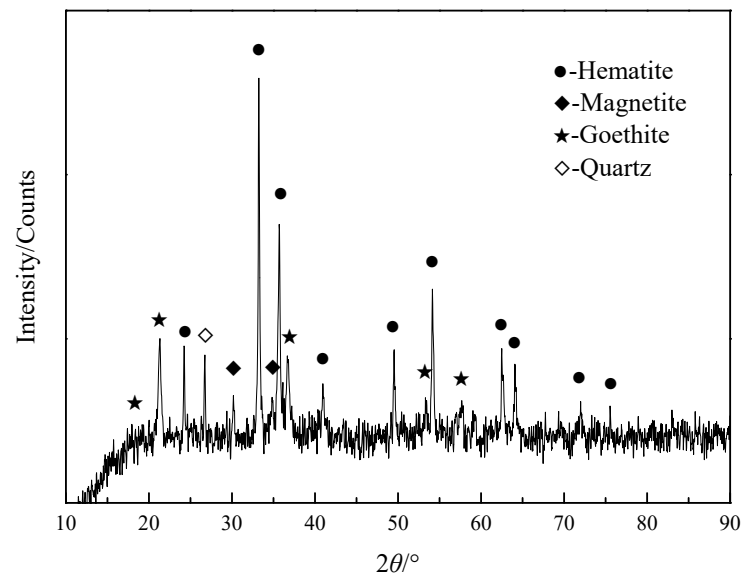
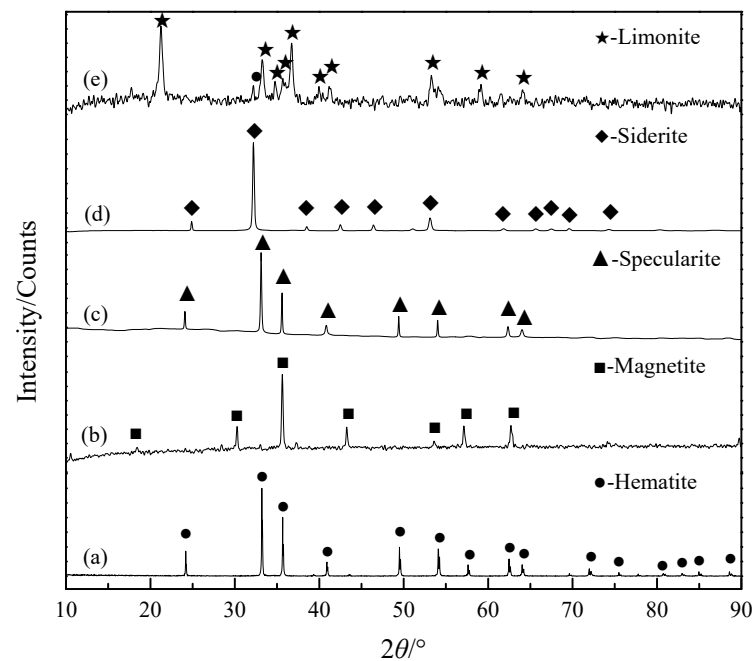
| Raw Materials | TFe | FeO | SiO_2 | CaO | Al_2O_3 | MgO | MnO_2 | V_2O_5 | LOI |
|----------------|-------|------|----------------|------|-------------------------|------|----------------|------------------------|------|
| Iron Ore Fines | 61.47 | 2.88 | 5.4 | 0.16 | 1.52 | 0.08 | 0.31 | 0.008 | 5.14 |

Table 2. Proximate and ultimate analyses of coal (air-dry basis)/wt.%.

| C | H | N | S | M_{ad} | A_{ad} | V_{ad} | F_{Cad} |
|-------|-------|-------|-------|----------|----------|----------|-----------|
| 83.73 | 0.725 | 0.645 | 0.186 | 1.45 | 15.06 | 3.63 | 79.86 |

Note: M_{ad} —moisture on air-dry basis; A_{ad} —ash on air-dry basis; V_{ad} —volatile matter on dry, ash-free basis; F_{Cad} —fixed carbon on air-dry basis.

XRD phase analysis of the iron ore fines and the several major iron-bearing pure minerals used in the experiment are shown in Figures 1 and 2. The results showed that the main phases of the iron ore fines were hematite, magnetite, goethite and quartz. It can be seen from Figure 2 that the purity of the hematite, magnetite, siderite, specularite and limonite was relatively high, allowing these materials to meet the requirements of this experiment.

**Figure 1.** XRD analysis of sintering iron ore fines.**Figure 2.** XRD analysis of iron-bearing pure minerals: (a) hematite; (b) magnetite; (c) specularite; (d) siderite; (e) limonite.

2.2. Experimental Apparatus and Method

Micro-sintering experiments were carried out using the experimental system of a tubular electric furnace with SiC heaters (Figure 3) (Changsha Kehui Furnace Technology Co., LTD., Changsha, China) [39]. Two kinds of gas were used in this experiment, O₂ (purity: 99.9 vol%) and N₂ (purity: 99.9 vol%); they were provided by Wuhan Minghui Gas Technology Co., LTD (Wuhan, China), and respectively configured using high-pressure gas cylinders, controlled with a glass rotor flowmeter and mixed with a mixer. They were then passed into the corundum tube (outer diameter: 80 mm, inner diameter: 70 mm, height: 1000 mm) in the tubular electric furnace and allowed to flow through the test sample in the crucible (outer diameter: 60 mm, inner diameter: 50 mm, height: 80 mm). A flue gas analyzer (MRU OPTIMA 7, Neckarsulm, Baden-Württemberg, Germany) was used to measure the gas composition at the entrance and exit of the reaction system. The measurement accuracy for O₂ and CO₂ was ±0.2%, and that for other gases was ±5 ppm.

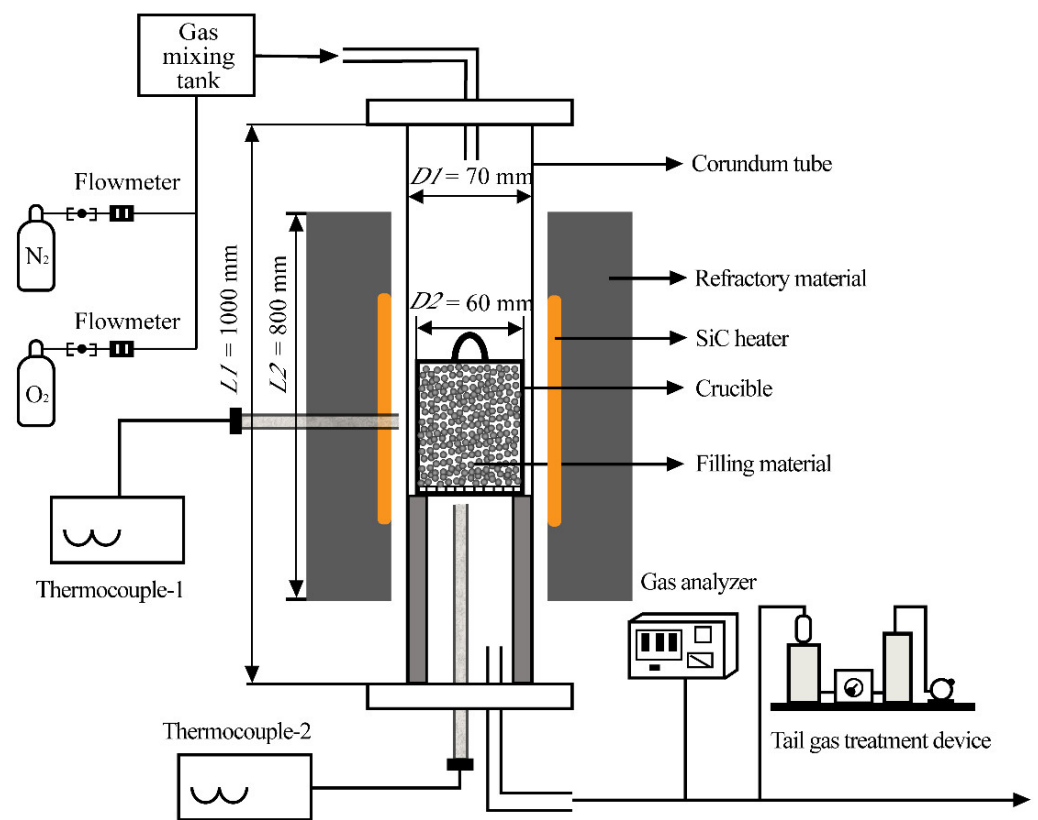


Figure 3. Schematic diagram of micro-sintering experiment apparatus.

A micro-sintering experiment device was used to simulate the process of producing nitrogen oxides in the test samples during sintering. The experiment steps were as follows: a dried sample of a certain quality was weighed and the sample placed into the test crucible (a crucible with holes at the bottom), then the heating program of the electric furnace was set. After the temperature in the corundum tube inside the electric furnace was stabilized to the temperature specified in the experiment, the crucible containing samples was placed in the corundum tube. Then, the corundum tube was sealed, the gas valve was opened and the gas composition controlled in terms of the air atmosphere (21% oxygen and 79% nitrogen) and gas flow (2 L/min). The gas flowed in from above the quartz tube, passed through the sample layer and flowed out from the below outlet. During the experiment, a flue gas analyzer was used to measure the flue gas composition in real time, and the data were recorded every 5 s. The reaction temperature was 1100 °C, the amount of pulverized coal in each group was 3 g and the amount of iron-containing pure mineral was 3 g.

2.3. Characterization Methods

The chemical compositions of the raw ore were determined with a wavelength dispersive X-ray fluorescence spectrometer (XRF, Rigaku/ZSXPrimus IV) and ICP-AES (Optima 2000DV). The crystalline phase compositions of the materials were detected with an X-ray diffractometer (XRD, D/Max-2500, Rigaku Co., Tokyo, Japan). Proximate analysis of coal was conducted according to the Chinese standard GB/T212-2008. SEM was conducted using a JEOL JSM-6610 scanning electron microscope (JEOL, Tokyo, Japan). The settings for the microscopy were EHT = 20 kV and I probe = 200 pA.

During the micro-sintering experiment, the compositions of the flue gas were detected online, and the peak concentration of NO_x , the relative influence factors for the peak concentration of NO_x and the relative emission rate of NO_x were analyzed and calculated. The calculation formulas are shown in Equations (1) and (3):

$$P_{\text{NO}_x} = \frac{X'_{\text{NO}_x}}{X^0_{\text{NO}_x}} \quad (1)$$

where $P_{(\text{NO}_x)}$ indicates the relative influence factors for the peak concentration of NO_x , $X^0_{\text{NO}_x}$ is the peak concentration of NO_x in pulverized coal combustion flue gas (10^{-6} (ppm)) and X'_{NO_x} is the peak concentration of NO_x in the flue gas for roasted samples.

By integrating the NO_x volume fractions corresponding to each moment, the total amount of NO_x generated during the coal combustion process can be obtained. The calculation formula is given in Equation (2):

$$E_{\text{NO}_x} = \frac{Q}{60} \times \int_a^b \varphi_{\text{NO}_x} \times 10^{-6} dt \times \frac{1000M}{22.4} \quad (2)$$

where E_{NO_x} is the NO_x emission in the flue gas for roasted samples (mg), Q is the flow rate of the flue gas (L/min), a and b are the beginning and end moments (s), φ_{NO_x} is the volume fraction of NO_x (10^{-6} (ppm)), t is the time (s) and M is the NO_x molar mass (g/mol).

Equation (3) is as follows:

$$R_{\text{NO}_x} = \frac{E'_{\text{NO}_x}}{E^0_{\text{NO}_x}}, \quad (3)$$

where R_{NO_x} is the relative emission rate of NO_x , $E^0_{\text{NO}_x}$ is the total nitrogen oxide emissions from coal combustion flue gas (mg) and E'_{NO_x} is the total NO_x emissions from the combustion flue gas of coal with iron-containing pure minerals added (mg).

3. Results

3.1. Effect of Iron Ore Fines on NO_x Emission Characteristics in Pulverized Coal Combustion

It can be seen from Figure 4a and Table 3 that, at the roasting temperature of 1100 °C, the pulverized coal rapidly burned to form nitrogen oxides, reached a peak value of about 244 ppm at 3.2 min, then decreased rapidly and dropped to zero after a period of time. The peak concentration of nitrogen oxides in the flue gas produced by the high-temperature roasting of the iron ore fines was only 30 ppm, indicating that the iron ore fines contained small amounts of nitrogen-containing compounds. When iron ore fines were added, the peak concentration of NO_x produced in the pulverized coal combustion increased from 244 ppm to 515 ppm, indicating that the iron ore fines had a relatively large enhancement effect on the NO_x emission rate in the pulverized coal combustion. It can be concluded from the relative emission rate of NO_x that mixing iron ore can greatly enhance the conversion rate for the total N- NO_x in pulverized coal, which increases the total emissions of NO_x in the flue gas. According to the analysis in Figure 4b–d, the addition of mixed iron ore reduced the concentration of oxygen and increased the concentration of carbon dioxide during the combustion of the pulverized coal, indicating that the addition of mixed iron ore could accelerate the combustion rate of the pulverized coal, the consumption rate of oxygen

and the generation rate of carbon dioxide. At the same time, the concentration of carbon monoxide in the flue gas decreased with the addition of the mixed iron ore, indicating that the addition of the mixed iron ore encouraged the full combustion of the pulverized coal.

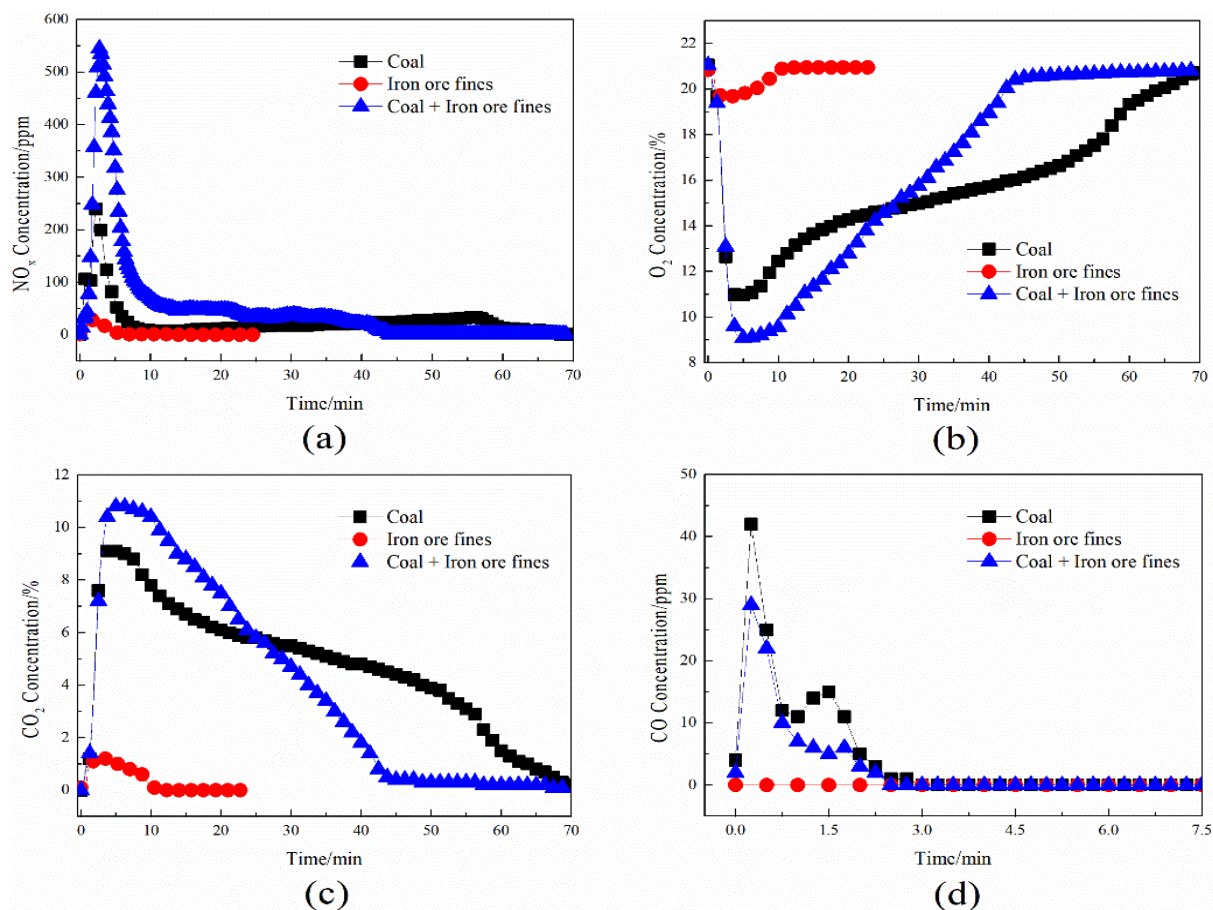


Figure 4. Effects of iron ore fines on flue gas composition characteristics in pulverized coal combustion: (a) NO_x concentration, (b) O_2 concentration, (c) CO_2 concentration, (d) CO concentration.

Table 3. Effects of iron ore fines on flue gas composition characteristics in pulverized coal combustion.

| Test Conditions | $X_{(\text{NO}_x)}/\text{ppm}$ | $P_{(\text{NO}_x)}$ | $R_{(\text{NO}_x)}$ |
|----------------------------------------------------------------------------------------------|--------------------------------|---------------------|---------------------|
| Coal | 244 | 1 | 1.00 |
| Iron ore fines | 30 | 0.12 | 0.05 |
| Coal and iron ore fines (minus the amount of NO_x produced by iron ore fines) | 515 | 2.11 | 1.89 |

3.2. Variation in Flue Gas Components during Oxidative Roasting of Iron-Bearing Pure Minerals

It can be seen from Figure 5 and Table 4 that a single piece of iron-containing pure mineral produced a portion of the nitrogen oxides during the roasting process, and the amount of NO_x produced was less than that from a single pulverized piece of coal. The order of the peak concentrations of nitrogen oxides in the roasting flue gas of the pure iron-bearing minerals was limonite > siderite > magnetite > hematite > specularite. The NO_x generation from specularite and hematite was very small, and the $P_{(\text{NO}_x)}$ and $R_{(\text{NO}_x)}$ values did not exceed 0.04. The roasting flue gas of siderite and magnetite contained certain amounts of NO_x . The $P_{(\text{NO}_x)}$ and $R_{(\text{NO}_x)}$ values were 0.11, 0.11, 0.12 and 0.05, respectively. However, the amount of NO_x produced by limonite was relatively large, reaching more than 50 ppm, and the $P_{(\text{NO}_x)}$ and $R_{(\text{NO}_x)}$ values were 0.21 and 0.12.

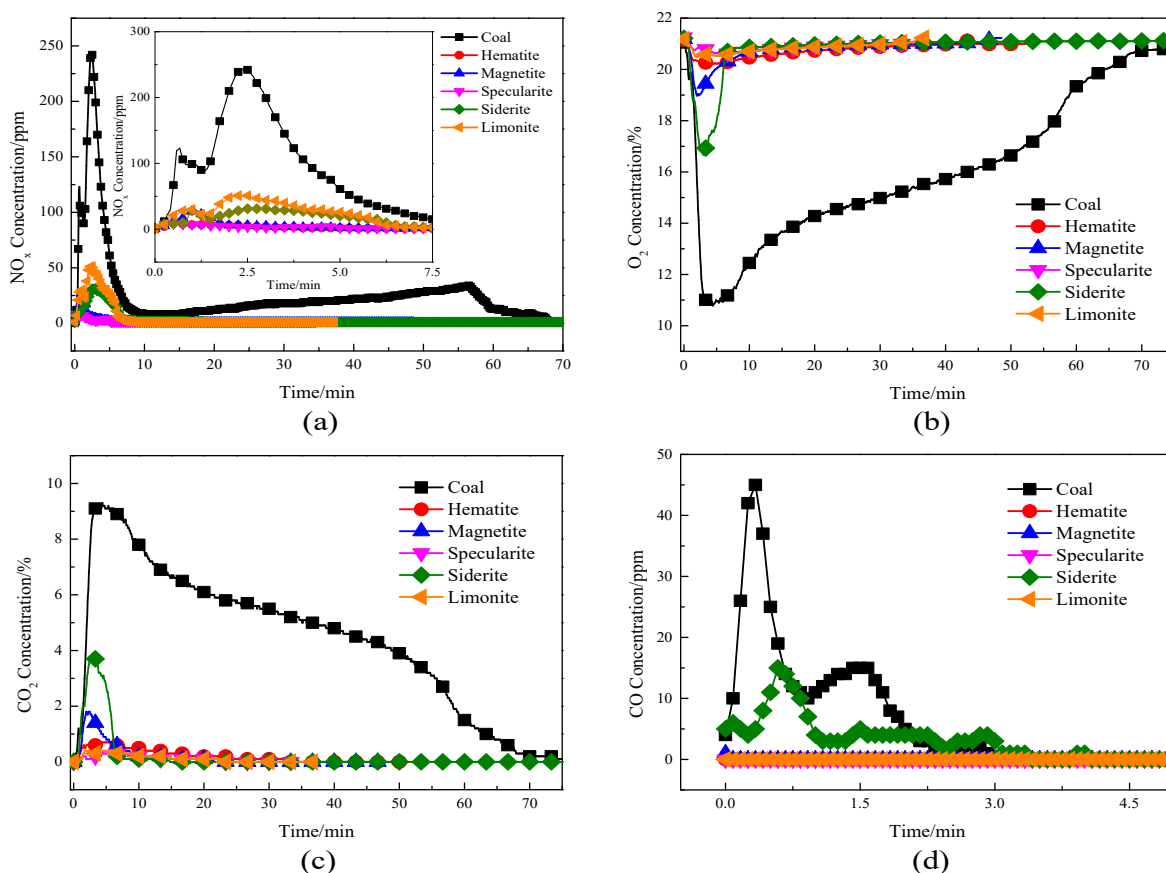


Figure 5. Emission characteristics of flue gas components during oxidative roasting of iron-bearing pure minerals. (a) NO_x concentration, (b) O_2 concentration, (c) CO_2 concentration, (d) CO concentration.

Table 4. List of $X_{(\text{NO}_x)}$, $P_{(\text{NO}_x)}$ and $R_{(\text{NO}_x)}$ values during oxidative roasting of iron-bearing pure minerals.

| Test Conditions | $X_{(\text{NO}_x)}$ /ppm | $P_{(\text{NO}_x)}$ | $R_{(\text{NO}_x)}$ |
|-----------------|--------------------------|---------------------|---------------------|
| Coal | 244 | 1 | 1.00 |
| Hematite | 9 | 0.04 | 0.04 |
| Magnetite | 27 | 0.11 | 0.05 |
| Specularite | 9 | 0.04 | 0.03 |
| Siderite | 28 | 0.11 | 0.12 |
| Limonite | 51 | 0.21 | 0.12 |

Figure 5b–d show that, during the roasting process of a single piece of iron-bearing pure mineral, siderite was oxidized and decomposed at a high temperature, consuming a certain amount of oxygen and at the same time generating a portion of the carbon dioxide and carbon monoxide, while magnetite was oxidized by oxygen at a high temperature and consumed only a small amount of oxygen. Limonite, hematite and magnetite iron ore had very little effect on the concentrations of oxygen and carbon dioxide during the roasting process.

3.3. Influence of Iron-Bearing Pure Minerals on NO_x Emission Characteristics in Pulverized Coal Combustion

A comparison of Figures 5a, 6a and 7 and Tables 4 and 5 shows that the types of iron-containing pure minerals had a great impact on the combustion rate of the pulverized coal and the generation and emission rates of NO_x in the combustion process. Through a comparison between the flue gas composition in iron-containing pure mineral roasting and that in catalytic pulverized coal combustion using iron-containing pure minerals at 1100°C ,

it can be seen that limonite had the greatest catalytic effect on the NO_x generation reaction during the pulverized coal combustion, and its $P_{(\text{NO}_x)}$ and $R_{(\text{NO}_x)}$ values reached 2.20 and 1.40, respectively, indicating that limonite can greatly enhance the NO_x generation rate and the N- NO_x conversion rate in pulverized coal combustion. The addition of hematite and specularite resulted in $p_{(\text{NO}_x)}$ and $R_{(\text{NO}_x)}$ reaching 1.63 and 1.37, and 1.26 and 1.02, respectively, indicating that hematite and specularite can improve the NO_x generation and conversion rates in pulverized coal combustion at the same time. The catalytic effects of siderite and magnetite on the NO_x formation reaction in pulverized coal combustion were weak, with $P_{(\text{NO}_x)}$ and $R_{(\text{NO}_x)}$ reaching 1.31 and 1.23, 0.97 and 0.84, respectively, indicating that the addition of siderite and magnetite improved the NO_x generation rate in pulverized coal combustion but inhibited N- NO_x conversion to a certain extent. The addition of siderite and magnetite reduced the $R_{(\text{NO}_x)}$ of pulverized coal combustion by 2.77% and 15.69%, respectively.

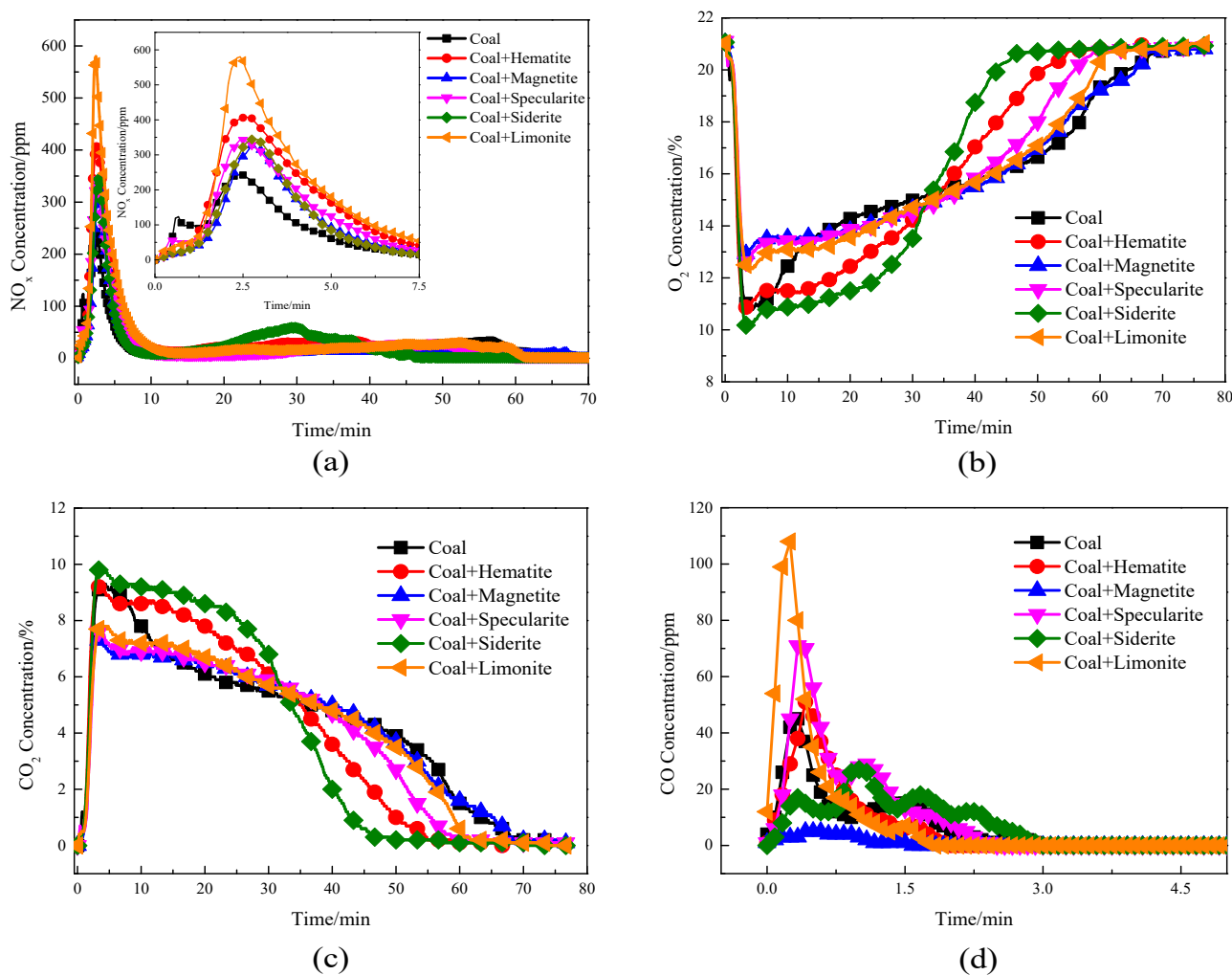


Figure 6. Influence of iron-bearing pure minerals on the variation law for flue gas composition in pulverized coal combustion: (a) NO_x concentration, (b) O_2 concentration, (c) CO_2 concentration, (d) CO concentration.

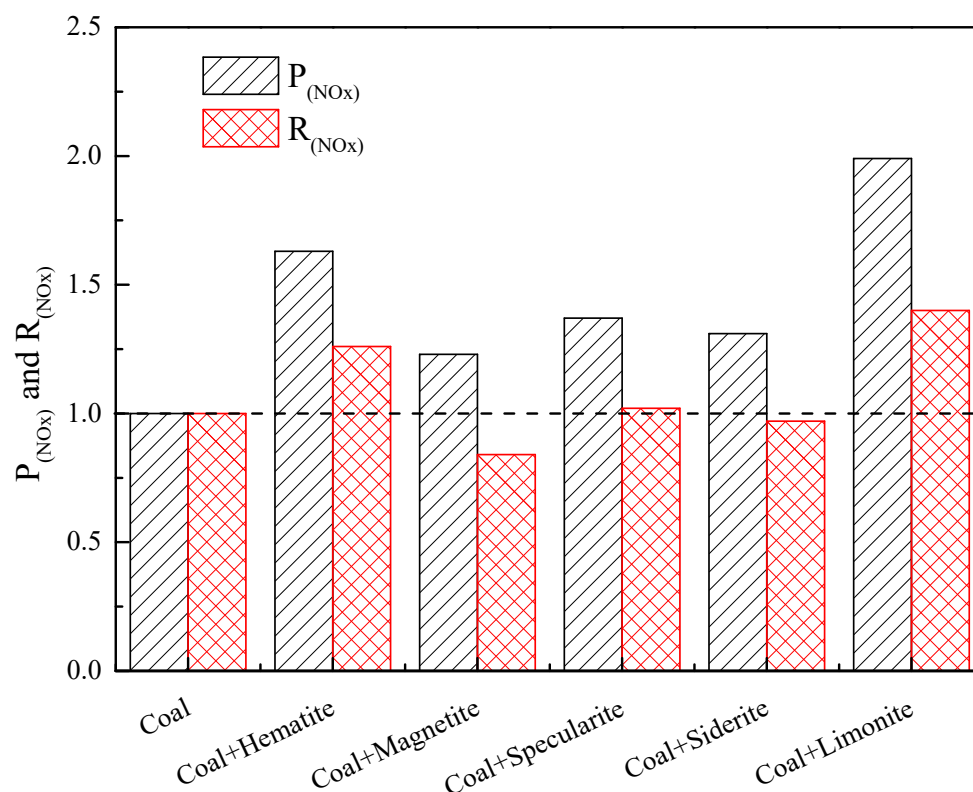


Figure 7. Effects of iron-bearing pure minerals on $P_{(\text{NO}_x)}$ and $R_{(\text{NO}_x)}$ during pulverized coal combustion.

Table 5. Effects of iron-bearing pure minerals on $X_{(\text{NO}_x)}$, $P_{(\text{NO}_x)}$ and $R_{(\text{NO}_x)}$ during pulverized coal combustion (minus the amount of NO_x produced by the iron-bearing pure minerals).

| Test Conditions | $X_{(\text{NO}_x)}/\text{ppm}$ | $P_{(\text{NO}_x)}$ | $R_{(\text{NO}_x)}$ |
|--------------------|--------------------------------|---------------------|---------------------|
| Coal | 244 | 1 | 1.00 |
| Coal + Hematite | 408 | 1.63 | 1.26 |
| Coal + Magnetite | 327 | 1.23 | 0.84 |
| Coal + Specularite | 343 | 1.37 | 1.02 |
| Coal + Siderite | 346 | 1.31 | 0.97 |
| Coal + Limonite | 537 | 1.99 | 1.40 |

According to the comparison of Figure 5b,c and Figure 6b,c, the addition of pure minerals containing iron reduced the contact between the coal and the air, resulting in an overall reduction in coal combustion speed, an increase in oxygen concentration and a decrease in carbon dioxide concentration. At the same time, the combustion cycle of the coal was shortened to varying degrees. The addition of siderite reduced the oxygen concentration in the combustion flue gas of the coal and increased the carbon dioxide concentration, which may have been due to the decomposition of the siderite, resulting in the simultaneous generation of carbon dioxide and consumption of part of the oxygen. Figure 6d shows that the addition of limonite, specularite and hematite increased the CO concentration and the total amount of CO generated from the combustion of coal, while siderite and magnetite increased the amount of CO in the flue gas of the coal combustion. The CO concentration decreased. Magnetite greatly reduced the CO concentration and the total amount of CO in the coal combustion flue gas, and siderite decreased the CO concentration in the coal combustion flue gas but the total amount and emission period increased. This was largely due to some of the CO being generated from the slow decomposition of siderite at high temperatures.

4. Discussion

Figure 8 shows the XRD patterns for the different combustion residues of pulverized coal with different kinds of iron-containing pure minerals added. It can be seen that the phase compositions of single pulverized coal combustion residues mainly consisted of $\text{Fe}_2(\text{SiO}_4)$, $\text{CaAl}_2(\text{SiO}_4)_2$, Al_2SiO_5 , SiO_2 , Al_2O_3 , Fe_2O_3 , etc. The phase composition of the pulverized coal combustion residues with iron-containing pure minerals mainly consisted of iron oxide. The main phase of the pulverized coal combustion residues with pure hematite mineral added was Fe_2O_3 , but it also contained small amounts of $\text{Fe}_2(\text{SiO}_4)$, $\text{CaAl}_2(\text{SiO}_4)_2$, Al_2SiO_5 , etc. The main phases of the pulverized coal combustion residues with pure magnetite mineral added were Fe_2O_3 and Fe_3O_4 , and a small amount of Al_2SiO_5 was also detected. The main phase of the pulverized coal combustion residues with pure specularite mineral added was Fe_2O_3 , and there was also a small amount of Al_2SiO_5 , etc. The main phases of the pulverized coal combustion residues with pure siderite mineral added were Fe_2O_3 and Fe_3O_4 , and a small amount of Al_2SiO_5 was also detected. The main phase of the pulverized coal combustion residue with pure limonite mineral added was Fe_2O_3 . In addition, it also contained small amounts of Al_2SiO_5 and $\text{CaAl}_2(\text{SiO}_4)_2$.

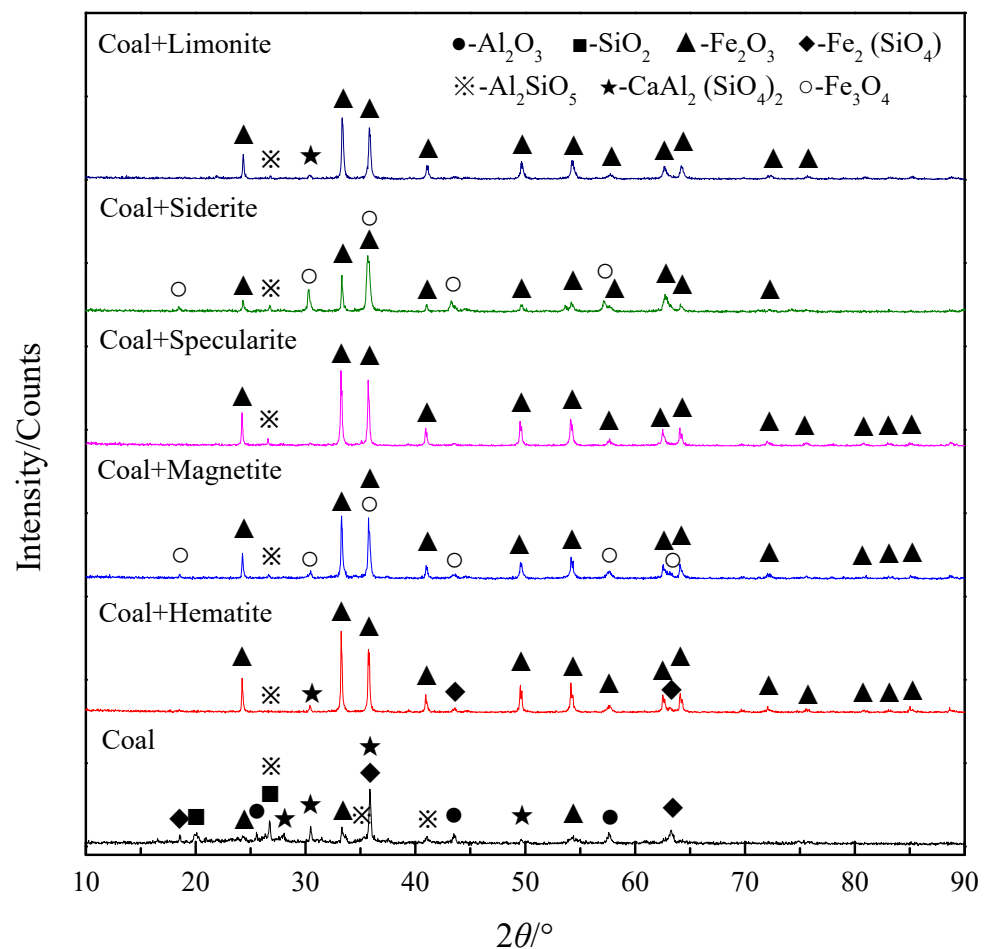


Figure 8. XRD patterns for pulverized coal combustion residues with different iron-containing pure minerals added.

Figure 9 shows SEM images of pulverized coal combustion residues with different kinds of iron-containing pure minerals added. It indicates that, with the addition of iron-containing pure minerals, the combustion residues of the mixture increased greatly, most of which were the roasting products of the iron-containing pure minerals, which adhered to the surface of the pulverized coal during the pulverized coal combustion, so that the pulverized coal did not fully burn.

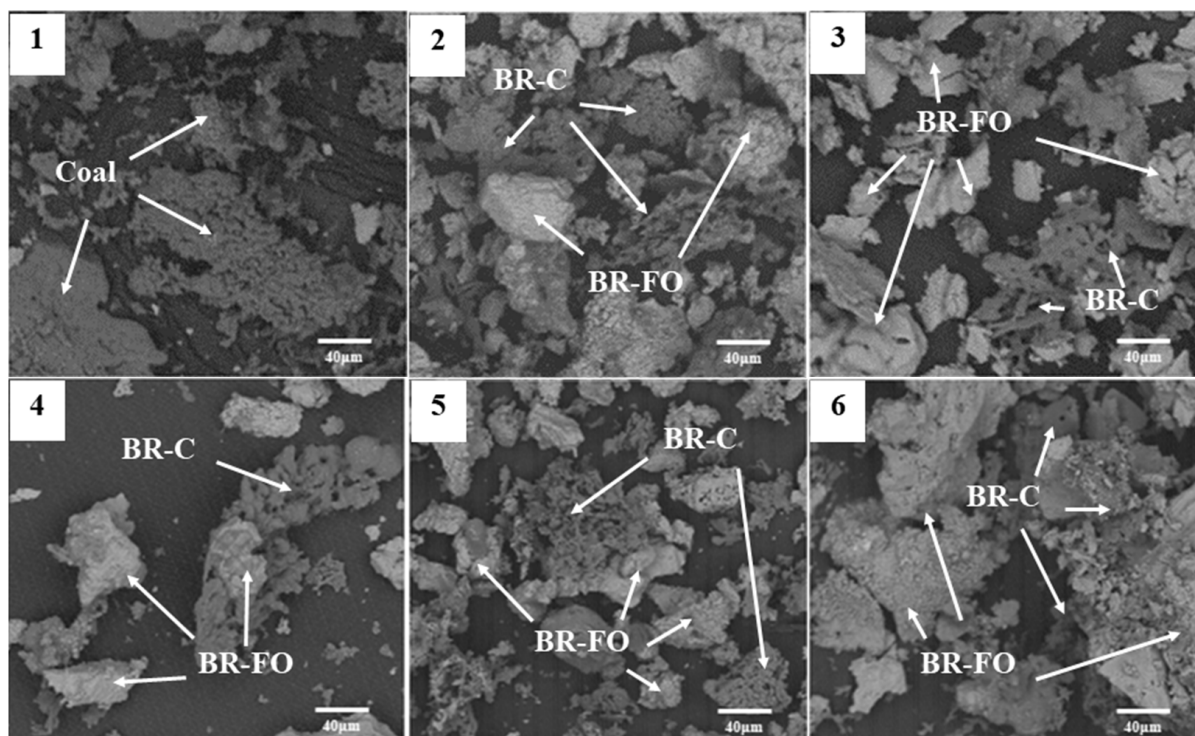


Figure 9. SEM images of pulverized coal combustion residues with different iron-containing pure mineral additions. BR-C: pulverized coal combustion residues; BR-FO: iron-containing pure mineral roasting residues. 1—pulverized coal; 2—pulverized coal and hematite; 3—pulverized coal and magnetite; 4—pulverized coal and specularite; 5—pulverized coal and siderite; 6—Pulverized coal and limonite.

As can be seen from Section 3.3, the peak NO_x concentration and the total NO_x emissions in the flue gas increased significantly after the pure minerals containing high-valence iron elements (limonite, hematite and specularite) were added to the pulverized coal. At the same time, the concentration of CO_2 in the flue gas decreased, the generation cycle of the CO_2 was shortened and the concentration and total emissions of CO increased. According to the analysis of Figures 8 and 9, with the addition of pure minerals containing high-valence iron elements, the combustion residues of the mixture increased greatly, and most were the roasting products of the iron-containing pure minerals, which adhered to the surface of the pulverized coal during combustion so that the pulverized coal did not fully burn, resulting in a decrease in CO_2 concentration and an increase in CO concentration in the flue gas. However, the peak value for the NO_x concentration in the flue gas increased significantly, indicating that the addition of pure minerals containing high-valence iron elements reduced the combustion performance of the pulverized coal and catalyzed the formation reaction of NO_x in the pulverized coal. Limonite contains crystal water, which evaporates rapidly and forms water vapor during high-temperature roasting. On the one hand, the existence of the water vapor promoted the combustion of the pulverized coal and the generation of NO_x . On the other hand, the evaporation of the crystal water led to the formation of many pores on the mineral surface, increased the reaction contact area between the dehydrated iron-bearing minerals and the pulverized coal and enhanced the catalytic effect of Fe_2O_3 on the NO_x formation reaction during the pulverized coal combustion. The catalytic effects of hematite and specularite on NO_x formation during pulverized coal combustion mainly resulted from the effective catalytic component Fe_2O_3 contained in the pure minerals.

The peak value for the NO_x concentration in the flue gas increased to a certain extent after the addition of pure minerals (magnetite and siderite) containing low-valence iron elements into the pulverized coal, while the total emissions decreased. The addition of

magnetite reduced the concentration of CO₂ in the pulverized coal combustion flue gas, shortened the generation cycle of the CO₂ and reduced the concentration of CO. This may have been due to the reaction of the CO in the flue gas and the NO_x at the combustion interface to produce N₂ and CO₂. Similarly, magnetite can react with NO to produce N₂ at high temperatures. When siderite was added to the pulverized coal, due to its own thermal decomposition under high temperature conditions to produce CO₂ and Fe₃O₄, the CO₂ concentration in the overall flue gas increased and the generation cycle of the CO₂ was greatly shortened, but the CO concentration decreased. This may have been due to the reaction between the CO in the flue gas and the NO_x at the combustion interface to produce N₂ and CO₂. Moreover, the Fe₃O₄ produced by siderite thermal decomposition could react with NO to produce N₂ under high temperature conditions. As can be seen from Figures 8 and 9, with the addition of pure minerals containing low-valence iron elements, a large number of combustion residues adhered to the surface of the pulverized coal during combustion, most of which were the roasting products of the iron-containing pure minerals, so that the pulverized coal did not fully burn. Moreover, the peak value for the NO_x concentration in the flue gas increased, but the total emissions decreased. This was because the addition of pure minerals containing low-valence iron elements reduced the combustion performance of the pulverized coal. Fe₃O₄ and CO in the system could react with NO_x to produce Fe₂O₃, N₂ and CO₂, and then Fe₂O₃ continued to catalyze the formation reaction of NO_x during the pulverized coal combustion [33].

To sum up, the type and composition of iron ore powder have a significant impact on the generation and emission of NO_x in the pulverized coal combustion process. In the actual process of iron ore sintering, iron ore fines and pulverized coal are fully mixed and granulated in the process of mixing and granulating. Therefore, controlling and adjusting the type and composition of the iron-containing raw materials in the mixture and the distribution of the iron-containing raw materials and the pulverized coal makes it possible to control the generation of NO_x in the pulverized coal combustion process to a certain extent, thereby regulating the emission of NO_x across the whole sintering process and achieving the purpose of NO_x emission reduction. Moreover, the addition of magnetite and siderite can be conducive to the reduction of nitrogen oxide emissions in iron ore sintering flue gas. Magnetite can also release heat in the sintering process, reduce the sintering carbon content, reduce sintering solid fuel consumption and pollutant emissions and help to improve the quality of sinter.

5. Conclusions

Iron ore fines can improve the NO_x emission rate and increase the total NO_x emissions during coal combustion. At the same time, they can accelerate the combustion rate of coal and stimulate its full combustion.

The type and composition of iron ore fines have a significant impact on the generation and emission of NO_x in the coal combustion process. With the addition of limonite, hematite or specularite, the peak concentration and total emissions of NO_x in the flue gas increased significantly, indicating that the addition of limonite, hematite and specularite reduce the combustion performance of coal and catalyze the formation of NO_x. With the addition of magnetite or siderite, the peak value for the NO_x concentration in the flue gas increased, but the total emissions decreased.

The generation of NO_x in the sintering process can be controlled to a certain extent by adjusting the type of iron-containing raw materials and the distribution of the iron-containing raw materials and coal. Moreover, the addition of magnetite is conducive to reducing emissions of NO_x from coal combustion in the process of iron ore sintering. Moreover, magnetite can release heat during sintering, which can help reduce the consumption of solid fuel, reduce pollutant emissions and improve the quality of sinter.

Author Contributions: Conceptualization, T.C. and X.Z.; methodology, J.W. and L.L.; software, J.W.; validation, T.C., X.Z. and B.S.; formal analysis, Z.W.; resources, T.C.; data curation, J.W. and J.L.; writing—original draft preparation, J.W.; writing—review and editing, T.C., X.Z. and L.L.; project administration, X.Z.; funding acquisition, B.S. and Z.W. All authors have read and agreed to the published version of the manuscript.

Funding: This research was funded by the Basic Research Fund of Zhongye Changtian International Engineering Co., Ltd. (grant number 2020JCYJ06).

Data Availability Statement: Data presented in this article are available on request from the corresponding author.

Acknowledgments: Thanks to the Analysis and Testing Center of Wuhan University of Science and Technology for providing technical support for this research work.

Conflicts of Interest: The authors declare no conflict of interest.

References

1. Rocha, L.; Kim, H.; Lee, C.; Jung, S.M. Mechanism of NO_x Formation from Nitrogen in the Combustion of the Coals Used in Sintering Process. *Metall. Mater. Trans. B* **2020**, *51*, 2068–2078. [[CrossRef](#)]
2. Zhu, T.Y. *Sintering Flue Gas Purification Technology*; Chemical Industry Press: Beijing, China, 2009; pp. 231–252.
3. Ni, W.; Li, H.; Zhang, Y.; Zou, Z. Effects of Fuel Type and Operation Parameters on Combustion and NO_x Emission of the Iron Ore Sintering Process. *Energies* **2019**, *12*, 213. [[CrossRef](#)]
4. Zhou, H.; Zhou, M.; Liu, Z.; Cheng, M.; Chen, J. Modeling NO_x emission of coke combustion in iron ore sintering process and its experimental validation. *Fuel* **2016**, *179*, 322–331. [[CrossRef](#)]
5. Chen, Y.; Guo, Z.; Wang, Z. Influence of CeO₂ on NO_x emission during iron ore sintering. *Fuel Process. Technol.* **2009**, *90*, 933–938. [[CrossRef](#)]
6. Ping, L.; Hao, J.; Wei, Y.; Zhu, X.; Xin, D. Effects of water vapor and Na/K additives on NO reduction through advanced biomass reburning. *Fuel* **2015**, *170*, 60–66.
7. Mukherjee, S. *Applied Mineralogy*; Springer: Dordrecht, Germany, 2011; pp. 428–489.
8. Chen, T.J. *Theory and Technology of Modern Sintering and Agglomeration*; Metallurgical Industry Press: Beijing, China, 2018.
9. Fan, X.; Zhao, Y.; Ji, Z.; Li, H.; Gan, M.; Zhou, H.; Chen, b.; Huang, X. New understanding about the relationship between surface ignition and low-carbon iron ore sintering performance. *Process Saf. Environ.* **2021**, *146*, 267–275. [[CrossRef](#)]
10. Speth, K.; Murer, M.; Spliethoff, H. Experimental Investigation of Nitrogen Species Distribution in Wood Combustion and Their Influence on NO_x Reduction by Combining Air Staging and Ammonia Injection. *Energy Fuels* **2016**, *30*, 5816–5824. [[CrossRef](#)]
11. Xu, M.X.; Li, S.Y.; Wu, Y.H.; Jia, L.S.; Lu, Q.G. Effects of CO₂ on the fuel nitrogen conversion during coal rapid pyrolysis. *Fuel* **2016**, *184*, 430–439. [[CrossRef](#)]
12. Gan, M.; Fan, X.; Lv, W.; Chen, X.; Ji, Z.; Jiang, T.; Yu, Z.; Zhou, Y. Fuel pre-granulation for reducing NO_x emissions from the iron ore sintering process. *Powder Technol.* **2016**, *301*, 478–485. [[CrossRef](#)]
13. Gan, M.; Ji, Z.; Fan, X.; Zhao, Y.; Chen, X.; Fan, Y. Insight into the high proportion application of biomass fuel in iron ore sintering through CO-containing flue gas recirculation. *J. Clean. Prod.* **2019**, *232*, 1335–1347. [[CrossRef](#)]
14. Wo, C.N. NO_x Formation of Pulverized Coal under Pressure Oxygen-Enriched Combustion. Master's Thesis, Zhejiang University, Hangzhou, China, 2020.
15. Lu, L. *Iron Ore: Mineralogy, Processing and Environmental Sustainability*; Elsevier: Amsterdam, The Netherlands, 2021; pp. 640–658.
16. Gan, M.; Fan, X.; Ji, Z.; Jiang, T.; Chen, X.; Yu, Z.; Li, G.; Yin, L. Application of biomass fuel in iron ore sintering: Influencing mechanism and emission reduction. *Ironmak. Steelmak. Processes Prod. Appl.* **2014**, *42*, 27–33. [[CrossRef](#)]
17. Mo, C.L.; Teo, C.S.; Hamilton, I.; Morrison, J. Admixing Hydrocarbons in Raw Mix to Reduce NO_x Emission in Iron Ore Sintering Process. *ISIJ Int.* **1997**, *37*, 350–357. [[CrossRef](#)]
18. Chen, Y.G.; Guo, Z.C.; Wang, Z. Application of Modified Coke to NO_x Reduction with Recycling Flue Gas during Iron Ore Sintering Process. *ISIJ Int.* **2008**, *11*, 1517–1523. [[CrossRef](#)]
19. Cheng, Z.L.; Wang, J.Y.; Wei, S.S.; Guo, Z.G.; Yang, J.; Wang, Q.W. Optimization of gaseous fuel injection for saving energy consumption and improving imbalance of heat distribution in iron ore sintering. *Appl. Energy* **2017**, *207*, 230–242. [[CrossRef](#)]
20. Yu, Z.Y.; Fan, X.H.; Gan, M.; Chen, X.L.; Lv, W. NO_x Reduction in the Iron Ore Sintering Process with Flue Gas Recirculation. *JOM* **2017**, *69*, 1570–1574. [[CrossRef](#)]
21. Locci, C.; Vervisch, L.; Farcy, B.; Domingo, P.; Perret, N. Selective Non-catalytic Reduction (SNCR) of Nitrogen Oxide Emissions: A Perspective from Numerical Modeling. *Flow Turbul. Combust.* **2017**, *100*, 301–340. [[CrossRef](#)]
22. Mahmoudi, S.; Baeyens, J.; Seville, J. NO_x formation and selective non-catalytic reduction (SNCR) in a fluidized bed combustor of biomass. *Biomass Bioenergy* **2010**, *34*, 1393–1409. [[CrossRef](#)]
23. Procházka, L.; Mec, P. Possibility of using fly ash after denitrification by SNCR as admixture in alkali-activated materials. *Mater. Today Proc.* **2021**, *37*, 42–47. [[CrossRef](#)]

24. Chen, X.P.; Liu, Q.; Wu, Q.; Luo, Z.K.; Zhao, W.T.; Chen, J.J.; Li, J.H. A hollow structure $\text{WO}_3\text{-CeO}_2$ catalyst for $\text{NH}_3\text{-SCR}$ of NO_x . *Catal. Commun.* **2021**, *149*, 106252. [[CrossRef](#)]
25. Jiang, B.Q.; Zhao, S.; Wang, Y.L.; Wenren, Y.S.; Zhang, X.M. Plasma-enhanced low temperature $\text{NH}_3\text{-SCR}$ of NO_x over a Cu-Mn/SAPO-34 catalyst under oxygen-rich conditions. *Appl. Catal. B Environ.* **2021**, *286*, 119886. [[CrossRef](#)]
26. Xu, G.Y.; Guo, X.L.; Cheng, X.X.; Yu, J.; Fang, B.Z. A review of Mn-based catalysts for low-temperature $\text{NH}_3\text{-SCR}$: NO_x removal and $\text{H}_2\text{O}/\text{SO}_2$ resistance. *Nanoscale* **2021**, *13*, 7052–7080. [[CrossRef](#)] [[PubMed](#)]
27. Carlos, L.; Moreno-Pirajan, J.C. Adsorption microcalorimetry Characterisation of activated carbons and their application in the study of NO_x retention. *J. Therm. Anal. Calorim.* **2015**, *121*, 245–255.
28. Song, Z.J.; Wang, B.; Yang, W.; Chen, T.; Sun, L. Research on NO and SO_2 removal using TiO_2 supported iron catalyst with vaporized H_2O_2 in a catalytic oxidation combined with absorption process. *Environ. Sci. Pollut. Res.* **2020**, *27*, 18329–18344. [[CrossRef](#)]
29. Morioka, K.; Inaba, S.; Shimizu, M.; Ano, K.; Sugiyama, T. Primary Application of the “In-Bed-de NO_x ” Process Using CaFe Oxides in Iron Ore Sintering Machines. *ISIJ Int.* **2000**, *40*, 280–285. [[CrossRef](#)]
30. Han, H.J.; Chen, Y.G.; Yu, F.M.; Li, J.L.; Wang, B.H. Simulation Investigation of NO Reduction by CO in Sintering Process. *Adv. Mater. Res.* **2013**, *781–784*, 2590–2593. [[CrossRef](#)]
31. Pan, J. Theoretical and Process Studies of the Abatement of Flue Gas Emissions during Iron Ore Sintering. Ph.D. Thesis, Central South University, Changsha, China, 2007.
32. Hao, Z.; Liu, Z.; Ming, C.; Zhou, M.; Liu, R. Influence of Coke Combustion on NO_x Emission during Iron Ore Sintering. *Energy Fuels* **2015**, *29*, 974–984.
33. Lv, W.; Fan, X.; Min, X.; Gan, M.; Chen, X.; Ji, Z. Formation of Nitrogen Mono Oxide (NO) during Iron Ore Sintering Process. *ISIJ Int.* **2017**, *58*, 236–243. [[CrossRef](#)]
34. Que, Z.; Ai, X. Effects of Iron Ores on the Combustion Behavior of Coke and NO_x Emission during Sintering Process. *ISIJ Int.* **2021**, *5*, 1412–1422. [[CrossRef](#)]
35. Cho, S.; Rocha, L.T.D.; Chung, B.J.; Jung, S.M. Effects of Adding Calcined Dolomite and Mill Scale to Sinter Mix on the Formation of NO and SO_2 in Iron Ore Sintering Process. *Metall. Mater. Trans. B* **2022**, *53*, 1936–1947. [[CrossRef](#)]
36. Que, Z.G.; Ai, X.B.; Wu, S.L. Reduction of NO_x emission based on optimized proportions of mill scale and coke breeze in sintering process. *Int. J. Miner. Metall. Mater.* **2021**, *28*, 1453–1461. [[CrossRef](#)]
37. Chen, Y.G.; Guo, Z.C.; Wang, Z. Simulation of NO Reduction by CO in Sintering Process. *J. Iron Steel Res.* **2009**, *21*, 6–9.
38. Sugimoto, Y.; Kawashima, H. Effect of demineralization and catalyst addition on N_2 formation during coal pyrolysis and on char gasification. *Fuel* **2003**, *82*, 2057–2064.
39. Shi, B.; Wan, J.; Chen, T.; Zhou, X.; Luo, Y.; Liu, J.; Hu, M.; Wang, Z. Study on Double-Layer Ignition Sintering Process Based on Autocatalytic Denitrification of Sintering Layer. *Minerals* **2022**, *12*, 33. [[CrossRef](#)]